A Comparative Study of Representative Categories of EBG Dielectric Quasi-Crystals

Alessandro Della Villa, Vincenzo Galdi, *Senior Member, IEEE*, Filippo Capolino, *Senior Member, IEEE*, Vincenzo Pierro, Stefan Enoch, and Gérard Tayeb

***Abstract*—This letter is concerned with a comparative study of the electromagnetic properties of two-dimensional, finite-size, aperiodically ordered "quasi-crystal" dielectric structures based on representative categories of "aperiodic-tiling" geometries. In this framework, a rigorous full-wave solver is used to explore the electromagnetic bandgap and directive radiation properties of potential interest in antenna applications.**

***Index Terms*—Aperiodic tilings, electromagnetic bandgap, quasi-crystals.**

I. Introduction

SINCE the seminal work by Yablonovitch [1], artificial materials capable of exhibiting electromagnetic bandgaps (EBG) have drawn a considerable interest from the microwave and antenna scientific communities, in view of the peculiar filtering and radiating effects attainable through their utilization. Classic designs are based on *periodic* (possibly defected) metallic or dielectric inclusions in a suitable host medium, and their rotational symmetries are accordingly bounded by the so-called "crystallographic restriction" [2]. The discovery in solid-state physics of "quasi-crystals" [3], [4], i.e., certain metallic alloys exhibiting X-ray diffraction spectra with "noncrystallographic" [e.g., 5-fold or $(K > 6)$-fold] symmetries that are known to be *incompatible* with spatial periodicity, has opened up intriguing perspectives toward *aperiodic* EBG quasi-crystals. During the past decade, several numerical and experimental studies have explored the properties of EBG quasi-crystals, in the form of one-dimensional (1-D) aperiodically stacked multilayers (see, e.g., [5]), two-dimensional (2-D) aperiodic arrays of cylindrical rods (see [6]–[14] for a sparse sampling), planar high-impedance substrates [15], and three-dimensional (3-D) structures fabricated via stereolithography [16]. Results have indicated the potential for a considerable broadening of the variety of properties already found in their periodic counterparts, in view of the additional degrees of freedom available in aperiodic geometries (see, e.g., the "bandgap engineering" in [17]). Specific applications have been suggested in a variety of fields, including lasers [18], negative refraction and subwavelength imaging [19], nonlinear optical frequency conversion [20], wavelength-division multiplexing [21], etc.

In this letter, with a view toward exploring how EBG quasi-crystals might open up new options in antenna applications, we address two aspects that appear to be still largely open.

1) A comparative study of the EBG properties of representative categories of 2-D finite-size dielectric quasi-crystals exhibiting different types and degrees of "order" and "symmetry," for given filling factor and dielectric contrast.
2) The exploration of possible applications to directive radiation.

II. Problem Statement and Geometry

We consider 2-D quasi-crystals composed of parallel infinitely long dielectric circular rods, with identical radius r and relative dielectric permittivity ϵ_r, placed in free space and excited by a transverse-magnetic EM field (i.e., electric field parallel to the rods) with implied time-harmonic $\exp(j\omega t)$ dependence. The spatial distribution of the rods is chosen according to certain representative classes of 2-D "aperiodic tilings" [2], i.e., arrangements of polygonal shapes ("tiles") devoid of any translational symmetry and capable of covering a plane without overlaps or gaps. Such geometries can be generated using various algorithms based essentially on three main procedures: *i)* juxtaposition of basic tiles with enforcement of suitable local "matching rules", *ii)* "cut-and-projection" schemes (from higher-dimensional periodic lattices), and *iii)* implementation of substitution rules (see [2] for more theoretical and implementation details, as well as computational aspects and tools). Although *aperiodic*, these geometries can still exhibit *order* and *symmetry* in a nontraditional sense. Typical attributes include [2]: Repetitiveness (i.e., occurrence of *any* bounded region of the whole tiling *infinitely often* across the tiling); short- and long-range order; statistical frequency of occurrence of the individual tiles; "noncrystallographic" rotational symmetries in local and/or weak (e.g., statistical) forms.

Fig. 1 displays the prototype quasi-crystal (cross-sectional) geometries of interest, generated by placing the cylindrical rods at the tile vertices within a square patch of the selected tiling, with size and scaling chosen so as to maintain the same total size and number of rods $(N = 256)$, the reference periodic crystal being a (16×16)-rod square [Fig. 1(a)]. Although not immediately discernible from Fig. 1, the chosen examples are

Manuscript received January 24, 2006; revised May 2, 2006.

A. Della Villa and F. Capolino are with the Department of Information Engineering, University of Siena, I-53100 Siena, Italy (e-mail: dellavilla@gmail.com; capolino@dii.unisi.it).

V. Galdi and V. Pierro are with the Waves Group, Department of Engineering, University of Sannio, I-82100 Benevento, Italy (e-mail: vgaldi@unisannio.it; pierro@unisannio.it).

S. Enoch and G. Tayeb are with the Institut Fresnel, CNRS 6133, Université Paul Cézanne Aix-Marseille III, Faculté des Sciences et Techniques, case 161, 13397 Marseille cedex 20, France (e-mail: stefan.enoch@fresnel.fr; gerard.tayeb@fresnel.fr).

Digital Object Identifier 10.1109/LAWP.2006.878904

representative of various types and degrees of order and symmetry. More specifically, the "thick-and-thin" Penrose tiling in Fig. 1(b) and the *binary* tiling in Fig. 1(c) are characterized by a 5-fold symmetry; the *octagonal* tiling in Fig. 1(e) is 8-fold symmetric; and the tilings in Fig. 1(d) and (f) exhibit 7-fold and 9-fold symmetry, respectively. With the exception of the *binary*, all tilings are characterized by a *purely discrete* spatial spectrum (indicative of long-range order), and are generated by algorithms amenable to cut-and-project schemes [2]. The *binary* tiling, generated via a substitution scheme [2], is known to exhibit a spatial spectrum with *singular continuous* character (indicative of a less-orderly spatial distribution). Also indicated in the figure caption is the average value d_{av} of the nearest-neighborhood distance $d_n = \min_{m \neq n} |\mathbf{r}_n^{(c)} - \mathbf{r}_m^{(c)}|$, between the rods centers $\mathbf{r}_n^{(c)}$, $n = 1, \ldots, N$. For all the quasi-crystal geometries in Fig. 1, the same rods radius is chosen, so as to maintain the same filling factor (defined as the ratio between the total area of the rods and the area of the host square).

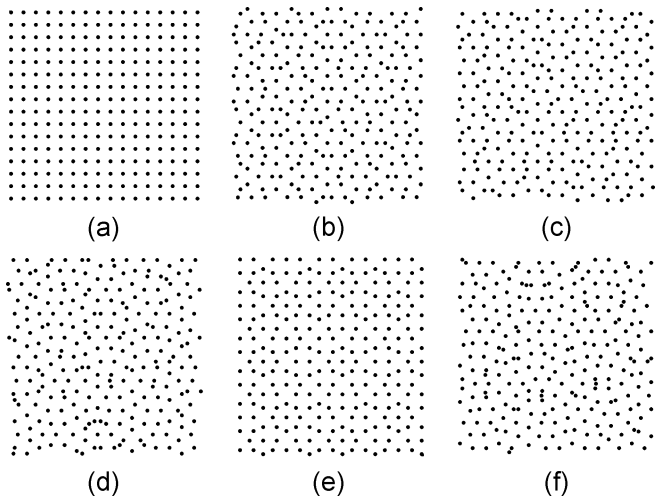

Fig. 1. Quasi-crystal geometries ($N = 256$ dielectric rods). (a) Periodic ($\mathrm{period} = a$); (b) Penrose "thick-and-thin" (5-fold symmetric, $d_{av} = 0.835a$); (c) *Binary* (5-fold symmetric, $d_{av} = 0.865a$); (d) 7-fold symmetric ($d_{av} = 0.840a$); (e) *Octagonal* (8-fold symmetric, $d_{av} = 0.915a$); (f) 9-fold symmetric ($d_{av} = 0.865a$).

III. Representative Results

A. EBG Observables and Results

For *finite-size* structures, EBG observables based on modal analysis or transmission coefficients are generally ill-defined and not necessarily physically meaningful. A physically sound observable to ascertain the EBG properties can be defined by considering the active power (per unit length) P_a radiated by a nonphased unit-amplitude electric line-source located inside the quasi-crystal. Bandgaps are accordingly defined as frequency ranges where radiation is strongly inhibited. By using the Poynting theorem, for a lossless structure, one obtains [22, p. 22]

$$P_a(\mathbf{r}_0, \omega) = -\frac{1}{2}\mathrm{Re}\{E(\mathbf{r}_0; \omega)\} = -\frac{\omega\mu_0}{2}\mathrm{Im}\{G(\mathbf{r}_0, \mathbf{r}_0; \omega)\}. \quad (1)$$

Here, $E(\mathbf{r}_0; \omega)$ denotes the electric field (directed along the longitudinal direction of the rods) radiated by the unit-amplitude line-current at $\mathbf{r}_0$, whilst $G(\mathbf{r}_0, \mathbf{r}_0; \omega)$ denotes the pertinent EBG Green's function evaluated at the source position. Such simple relations can be obtained because of the inherent *scalar* nature of the 2-D field problems treated here. Accordingly, we define as "radiativity" the normalized radiated power as

$$\rho(\mathbf{r}_0, \omega) = P_a(\mathbf{r}_0, \omega)/P_0(\mathbf{r}_0, \omega), \quad (2)$$

where $P_0 = \omega\mu_0/8$ [W/m] is the active power radiated by the unit-amplitude line-source in free space, so that $\rho(\mathbf{r}_0, \omega) = 1$ in the absence of the quasi-crystal. The observable in (2) closely resembles the *local density of states* (LDOS) [23] in solid-state physics. In our investigation, the computation of the Green's function in (2) is performed via a rigorous full-wave method, based on Fourier-Bessel multipolar field expansions [24], already applied successfully to the characterization of finite-size EBG crystals [23] and quasi-crystals [14]. To gain some insights into the underlying aperiodic-order-induced phenomenologies, we performed a comprehensive parametric study of the radiativity response of the quasi-crystal geometries in Fig. 1, for several combinations of the rods permittivity and filling factor values, and at various positions $\mathbf{r}_0$. Some representative results (for $\sim$7% filling factor, and $\epsilon_r = 6$, 12) are shown in Fig. 2. In these plots, the radiativity in (2) (computed at the center of the crystal, $\mathbf{r}_0 = \mathbf{0}$) is displayed as a function of the normalized frequency a/λ_0, with a denoting the period of the reference periodic crystal in Fig. 1(a), and λ_0 denoting the free-space wavelength. Bandgaps, identified by deep minima of the radiativity, can be observed for both permittivity values, though considerably more pronounced for the case $\epsilon_r = 12$. It is observed that, as compared with the periodic crystal, the quasi-crystals tend to exhibit a generally *richer* bandgap structure, which typically entails a main bandgap (moderately deeper than the periodic counterpart) plus certain secondary bandgaps at lower and higher frequencies. Moreover, as the symmetry order is increased, several in-band peaks (attributable to localized modes) tend to appear [cf. Fig. 2(d) and (f)]. The wave mechanisms underlying the formation of the various bandgaps are rather complex, and generally involve both long- and short-range interactions as well as multiple scattering phenomena. For the Penrose quasi-crystal in Fig. 1(b), we carried out a more detailed investigation of the first three bandgaps [14], from which the central and the higher-frequency bandgaps [see Fig. 2(b)] turned out to be related to Bragg-type conditions in the Fourier spatial spectrum of the quasi-crystals, whereas the lower-frequency bandgap turned out to stem from multiple scattering phenomena (see [14] for more details). Similar mechanisms, currently under investigation, are expected to take place for the other quasi-crystals. Overall, the results in Fig. 2 provide instructive insights into typical aperiodic-order-induced EBG effects. The trends analyzed in an idealized 2-D configuration serve to understand the bandgap behavior of realistic 3-D structures featuring unavoidable longitudinal truncations. The reader is referred to [25] for a comparison of the properties of 3-D crystals fabricated with finite-length rods and their 2-D idealized counterparts.

The example below illustrates a simple and promising application to directive radiation.

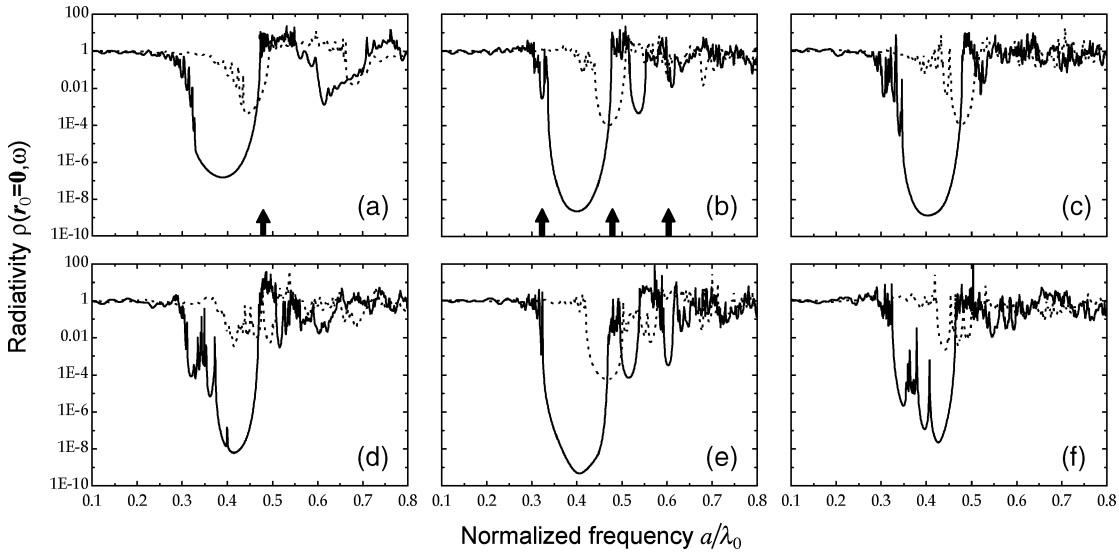

Fig. 2. Radiativity in (2) (logarithmic scale) computed at the center of the structure vs. normalized frequency a/λ_0 for the quasi-crystal geometries in Fig. 1 with $r = 0.3a$ (i.e., filling factor $= 7.07\%$). - - - $\epsilon_r = 6$; —— $\epsilon_r = 12$. Arrows indicate frequency values utilized for directive radiation (see Fig. 3).

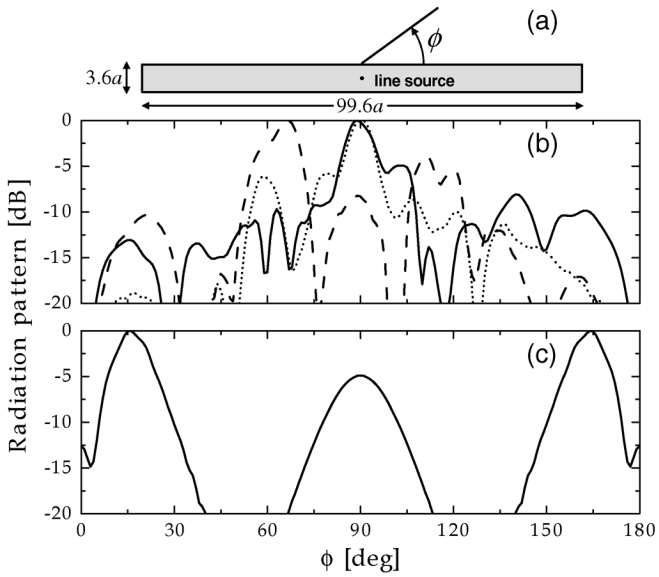

Fig. 3. (a) Schematic: electric line source located at the center of a (quasi-)crystal slab of size $99.6a \times 3.6a$ (400 dielectric rods with $r = 0.3a$ and $\epsilon_r = 12$). (b) Radiation patterns for the Penrose case. —— $a/\lambda_0 = 0.327$; - - - $a/\lambda_0 = 0.479$; $\cdots\cdots$ $a/\lambda_0 = 0.6$. (c) Radiation pattern for the periodic case $(a/\lambda_0 = 0.479)$.

B. Application Example: Directive Radiation From Penrose Quasi-Crystal Slabs

We consider an electric line source located at the center of a Penrose quasi-crystal slab made of size $99.6a \times 3.6a$, containing 400 dielectric rods of radius $r = 0.3a$ and relative permittivity $\epsilon_r = 12$ [see Fig. 3(a)]. Its radiation pattern (computed via the full-wave method in [24]) in the top halfspace is shown in Fig. 3(b) for three values of the normalized frequency for which some moderately directive behavior was observed. In particular, at frequency $a/\lambda_0 = 0.327$ and $a/\lambda_0 = 0.6$ one observes a maximum at broadside ($\phi = 90°$), whereas at $a/\lambda_0 = 0.479$ the maximum is shifted off broadside ($\phi \approx 70°$). Note that no attempt of parametric optimization was made at this preliminary stage, and the radiation patterns still exhibit high sidelobes. Nevertheless, a moderate directivity enhancement is clearly visible. The phenomenon of enhanced directivity has already been observed for sources located inside crystals composed of periodic lattices of metallic or dielectric rods (which have also been modeled as artificial dielectrics [26]). In [27]–[29], isotropic sources have been shown to produce high directivity when surrounded by grounded artificial dielectrics composed of periodic lattices of rods or grids, characterized by an effective relative permittivity less than unity. The possibility of achieving a narrow beam pointing off broadside was also theoretically predicted by the leaky-wave model in [27], [28], based on the seminal work in [30]. In [29], the high directivity at broadside was explained in terms of phase-matching conditions at the air-material interface for the plane-wave spectrum excited by the source. In [31], an alternative parameterization, capable of predicting quantitatively the amount of the directivity enhancement, was provided in terms of very fast and slowly attenuating leaky-waves excited by the source in the artificial dielectric slab. While all these studies were related to *periodic* crystals, this letter shows for the first time similar effects obtained with an *aperiodically ordered* quasi-crystal slab. As observed from Fig. 3(b), for the Penrose quasi-crystal, this effect can be obtained at *three* distinct frequencies which turn out to be close to the upper band-edges of the first two bandgaps and in the vicinity of the third bandgap [see the arrows in Fig. 2(b)]. Similar results, not shown for brevity, were observed for the other quasi-crystal geometries in Fig. 1. For the periodic counterpart, in a comparable frequency range, moderately enhanced directivity was achieved only at a *single* frequency [$a/\lambda_0 = 0.479$, see Fig. 3(c)] close to the upper band-edge of the only bandgap observable [see the arrow in Fig. 2(a)]. For the periodic case [27]–[29], [31], it was observed the dependence of the beam direction and width on the crystal slab thickness, and it was parameterized in terms of the propagation constant of the excited leaky wave [31]. Also in the present case, numerical simulations (not shown for brevity) indicate that the beam direction and width depend on the slab

thickness, and further investigations are needed to understand the possible role of leaky-wave phenomena. In the example presented, although no optimization effort was made, the slab thickness value $(3.6a)$ was chosen so as to provide reasonably directive radiation patterns. To sum up, the preliminary results above seem to indicate the potential usefulness of EBG quasi-crystals in antenna applications. In particular, the possibility of operating at *lower* ($\sim$68% of the periodic counterpart, for the Penrose case) and *multiple* frequencies could open up new perspectives for miniaturized and smart antennas. Clearly, further investigation is still needed to come up with design and optimization procedures.

IV. Conclusion

In this letter, a comparative study of the EM properties of 2-D finite-size dielectric EBG quasi-crystals has been addressed. Preliminary results concerning representative aperiodic-tiling geometries seem to indicate promising potentials for the use of EBG quasi-crystals in antenna applications. Current and future investigations are aimed at a better understanding of the wave mechanisms underlying the bandgap formation, as well as possible control and optimization mechanisms, to come up with potentially useful design rules for "bandgap engineering" and directive radiation.

References

[1] E. Yablonovitch, "Inhibited spontaneous emission in solid-state physics and electronics," *Phys. Rev. Lett.*, vol. 58, no. 20, pp. 2059–2062, May 1987.

[2] M. Senechal, *Quasicrystals and Geometry*. Cambridge, U.K.: Cambridge University Press, 1995.

[3] D. Shechtman, I. Blech, D. Gratias, and J. W. Cahn, "Metallic phase with long-range orientational order and no translation symmetry," *Phys. Rev. Lett.*, vol. 53, no. 20, pp. 1951–1953, Nov. 1984.

[4] D. Levine and P. J. Steinhardt, "Quasicrystals: a new class of ordered structures," *Phys. Rev. Lett.*, vol. 53, no. 26, pp. 2477–2480, Dec. 1984.

[5] E. Maciá, "Optical engineering with Fibonacci dielectric multilayers," *Appl. Phys. Lett.*, vol. 73, no. 23, pp. 3330–3332, Dec. 1998.

[6] Y. S. Chan, C. T. Chan, and Z. Y. Liu, "Photonic band gaps in two dimensional photonic quasicrystals," *Phys. Rev. Lett.*, vol. 80, no. 5, pp. 956–959, Feb. 1998.

[7] C. Jin, B. Cheng, B. Man, Z. Li, and D. Zhang, "Two-dimensional dodecagonal and decagonal quasiperiodic photonic crystals in the microwave region," *Phys. Rev. B*, vol. 61, no. 16, pp. 10 762–10 767, Apr. 2000.

[8] M. E. Zoorob, M. D. B. Charleton, G. J. Parker, J. J. Baumeberg, and M. C. Netti, "Complete photonic bandgaps in 12-fold symmetric quasicrystals," *Nature*, vol. 404, pp. 740–743, Apr. 2000.

[9] M. A. Kaliteevski, S. Brand, R. A. Abram, T. F. Krauss, R. M. De La Rue, and P. Millar, "Two-dimensional Penrose-tiled photonic quasicrystals: diffraction of light and fractal density of modes," *J. Mod. Opt.*, vol. 47, no. 11, pp. 1771–1778, Nov. 2000.

[10] X. Zhang, Z.-Q. Zhang, and C. T. Chan, "Absolute photonic band gaps in 12-fold symmetric photonic quasicrystals," *Phys. Rev. B*, vol. 63, no. 8, Feb. 2001. Paper no. 081105(R).

[11] M. Bayndir, E. Cubukcu, I. Bulu, and E. Ozbay, "Photonic bandgap effect, localization, and waveguiding in the two-dimensional Penrose lattice," *Phys. Rev. B*, vol. 63, no. 16, Apr. 2001. Paper no. 161104(R).

[12] M. Hase, H. Miyazaki, M. Egashira, N. Shinya, K. M. Kojima, and S. Uchida, "Isotropic photonic band gap and anisotropic structures in transmission spectra of two-dimensional fivefold and eightfold symmetric quasiperiodic photonic crystals," *Phys. Rev. B*, vol. 66, no. 21, Dec. 2002. Paper no. 214205.

[13] B. P. Hiett, D. H. Beckett, S. J. Cox, J. M. Generowicz, M. Molinari, and K. S. Thomas, "Photonic band gaps in 12-fold symmetric quasicrystals," *J. Mat. Sci.*, vol. 14, no. 5–7, pp. 413–416, May 2003.

[14] A. Della Villa, S. Enoch, G. Tayeb, V. Pierro, V. Galdi, and F. Capolino, "Bandgap formation and multiple scattering in photonic quasicrystals with a Penrose-type lattice," *Phys. Rev. Lett.*, vol. 94, no. 18, May 2005. Paper no. 183903.

[15] H. Q. Li, Z. H. Hang, Y. Q. Qin, Z. Y. Wei, L. Zhou, Y. W. Zhang, H. Chen, and C. T. Chan, "Quasiperiodic planar metamaterial substrates," *Appl. Phys. Lett.*, vol. 86, no. 12, Mar. 2005. Paper no. 121 108.

[16] W. Man, M. Megens, P. J. Steinhardt, and P. M. Chaikin, "Experimental measurement of the photonic properties of icosahedral quasicrystals," *Nature*, vol. 436, pp. 993–996, Aug. 2005.

[17] Y. Q. Wang, S. S. Jian, S. Z. Han, S. Feng, Z. F. Feng, B. Y. Cheng, and D. Z. Zhang, "Photonic bandgap engineering of quasiperiodic photonic crystals," *J. Appl. Phys.*, vol. 97, no. 10, May 2005. Paper no. 106112.

[18] M. Notomi, H. Suzuki, T. Tamamura, and K. Edagawa, "Lasing action due to the two-dimensional quasiperiodicity of photonic quasicrystals with a Penrose lattice," *Phys. Rev. Lett.*, vol. 92, no. 12, Mar. 2004. Paper no. 123906.

[19] Z. Feng, X. Zhang, Y. Wang, Z.-Y. Li, B. Cheng, and D.-Z. Zhang, "Negative refraction and imaging using 12-fold-symmetry quasicrystals," *Phys. Rev. Lett.*, vol. 94, no. 24, Jun. 2005. Paper no. 247402.

[20] R. Lifshitz, A. Arie, and A. Bahabad, "Photonic quasicrystals for nonlinear optical frequency conversion," *Phys. Rev. Lett.*, vol. 95, no. 13, Sep. 2005. Paper no. 133901.

[21] J. Romero-Vivas, D. N. Chigrin, A. V. Lavrinenko, and C. M. Sotomayor Torres, "Photonic quasicrystals for application in WDM systems," *Phys. Stat. Sol. A*, vol. 202, no. 6, pp. 997–1001, May 2005.

[22] R. F. Harrington, *Time-Harmonic Electromagnetic Fields*. New York: McGraw-Hill, 1961.

[23] A. A. Asatryan, K. Busch, R. C. McPhedran, L. C. Botten, C. Martijn de Sterke1, and N. A. Nicorovici, "Two-dimensional Green's function and local density of states in photonic crystals consisting of a finite number of cylinders of infinite length," *Phys. Rev. E*, vol. 63, no. 4, Apr. 2001. Paper no. 46612.

[24] D. Felbacq, G. Tayeb, and D. Maystre, "Scattering by a random set of parallel cylinders," *J. Opt. Soc. Amer. A*, vol. 11, no. 9, pp. 2526–2538, Sep. 1994.

[25] P. Sabouroux, G. Tayeb, and D. Maystre, "Experimental and theoretical study of resonant microcavities in two-dimensional photonic crystals," *Opt. Commun.*, vol. 160, no. 1–3, pp. 33–36, Feb. 1999.

[26] J. Brown, "Artificial dielectrics having refractive indices less than unity," *Proc. Inst. Elect. Eng.*, pt. IV, vol. 100, pp. 51–62, May 1953.

[27] K. C. Gupta, "Narrow-beam antennas using an artificial dielectric medium with permittivity less than unity," *Electron. Lett.*, vol. 7, no. 1, pp. 16–18, Jan. 1971.

[28] I. J. Bahl and K. C. Gupta, "A leaky-wave antenna using an artificial dielectric medium," *IEEE Trans. Antennas Propag.*, vol. 22, no. 1, pp. 119–122, Jan. 1974.

[29] S. Enoch, G. Tayeb, P. Sabouroux, N. Guérin, and P. Vincent, "A metamaterial for directive emission," *Phys. Rev. Lett.*, vol. 89, no. 21, Nov. 2002. Paper no. 213902.

[30] T. Tamir and A. A. Oliner, "The influence of complex waves on the radiation field of a slot-excited plasma layer," *IEEE Trans. Antennas Propag.*, vol. 10, no. 1, pp. 55–65, Jan. 1962.

[31] G. Lovat, P. Burghignoli, F. Capolino, D. R. Jackson, and D. R. Wilton, "Analysis of directive radiation from a line source in a metamaterial slab with low permittivity," *IEEE Trans. Antennas Propag.*, vol. 54, no. 3, pp. 1017–1030, Mar. 2006.